

Fadi Bou-Abdallah · Paolo Arosio · Sonia Levi
Christine Janus-Chandler · N. Dennis Chasteen

Defining metal ion inhibitor interactions with recombinant human H- and L-chain ferritins and site-directed variants: an isothermal titration calorimetry study

Received: 21 January 2003 / Accepted: 7 March 2003 / Published online: 5 April 2003
© SBIC 2003

Abstract Zinc and terbium, inhibitors of iron incorporation in the ferritins, have been used for many years as probes of structure-function relationships in these proteins. Isothermal titration calorimetric and kinetic measurements of Zn(II) and Tb(III) binding and inhibition of Fe(II) oxidation were used to identify and characterize thermodynamically (n , K , ΔH° , ΔS° , and ΔG°) the functionally important binding sites for these metal ions in recombinant human H-chain, L-chain, and H-chain site-directed variant ferritins. The data reveal at least two classes of binding sites for both Zn(II) and Tb(III) in human H-chain ferritin: one strong, corresponding to binding of one metal ion in each of the eight three-fold channels, and the other weak, involving binding at the ferroxidase and nucleation sites of the protein as well as at other weak unidentified binding sites. Zn(II) and Tb(III) binding to recombinant L-chain ferritin showed similar stoichiometries for the strong binding sites within the channels, but fewer weaker binding sites when compared to the H-chain protein. The kinetics and binding data indicate that the binding of Zn(II) and Tb(III) in the three-fold channels, which is the main pathway of iron(II) entry in ferritin, blocks the access of most of the iron to the ferroxidase sites on the interior of the protein, accounting for the strong inhibition by these metal ions of the oxidative deposition of iron in ferritin.

Keywords Ferritin · Iron oxidation · Isothermal titration calorimetry · Terbium binding · Zinc binding

Abbreviations HuHF and HuLF: recombinant human H-chain and L-chain ferritins · HoSF: horse spleen ferritin · ITC: isothermal titration calorimetry · Mes: 2-(*N*-morpholino)ethanesulfonic acid · Mops: 3-(*N*-morpholino)propanesulfonic acid · A2: nucleation site variant (E61A + E64A + E67A) · S9: outer opening to three-fold channel variant (H118A, K86Q) · S10: inner opening to three-fold channel variant (H128A, K86Q) · S14: three-fold channel variant (D131I + E134F) · 222: ferroxidase center variant (E62K + H65G and also K86Q)

Introduction

Ferritins are a class of iron biomineralizing proteins of both eukaryotes and prokaryotes. These proteins detoxify and store cellular iron in a biologically available form [1, 2, 3, 4, 5]. Mammalian ferritins are composed of two types of subunits, H (heavy, ~21,000 kDa) and L (light, ~20,000 kDa), that assemble to form a spherical protein shell with 4/3/2 octahedral symmetry, surrounding a central cavity containing up to 4500 iron atoms as a ferric hydrous oxide mineral core [3, 4, 5]. While the H-subunit is responsible for rapid oxidation of Fe(II) to Fe(III) at its ferroxidase center, the L-subunit appears to be important in facilitating iron hydrolysis and nucleation of the mineral core [6, 7]. The formation of a mineral core within the ferritin cavity is a multi-step process involving Fe(II) binding at the ferroxidase centers, oxidation of the ferrous complex by molecular oxygen, formation of a peroxo-Fe(III) dimer that decays to a μ -oxo-bridged diFe(III) complex(es), and finally nucleation and mineralization of the oxidized iron [3, 4, 5, 6, 7, 8, 9, 10].

The structure-function relationships and mechanisms of iron oxidation and mineralization in ferritins have been widely studied [3, 4, 5, 9, 10]. Ferritins of various

F. Bou-Abdallah · C. Janus-Chandler · N.D. Chasteen (✉)
Department of Chemistry,
University of New Hampshire,
Durham, NH, 03824, USA
E-mail: ndc@cisunix.unh.edu
Tel.: +1-603-8622520
Fax: +1-603-8624278

P. Arosio
Chemistry Section, Faculty of Medicine, University of Brescia,
25123 Brescia, Italy

S. Levi
Department of Biological and Technological Research,
Istituto di Ricovero e Cura a Carattere Scientifico (IRCCS)
H. San Raffaele, 20132 Milan, Italy

types, e.g. animal versus bacterial, exhibit different mechanisms for iron binding, oxidation, and mineralization. Most data indicate that iron enters the cavity of animal ferritins via the eight hydrophilic three-fold channels [11, 12, 13, 14, 15]. Molecular diffusion studies in horse spleen ferritin (HoSF) and human H-chain ferritin (HuHF) reinforce this conclusion and illustrate the permeability of the protein shell to small molecules via the three-fold channels [16, 17]. More recently, a thermodynamic study has confirmed the three-fold channels as iron(II) pathways into human ferritin and has indicated that alterations of the conserved amino acid residues that line these channels (i.e. Asp131 and Glu134) decrease the capacity of H-chain ferritins to bind Fe(II) [18].

Binding experiments using Mn(II), VO(IV), Cd(II), Zn(II), and Tb(III) have shown that these metal ions compete with Fe(II) and Fe(III) and with one another, implying some common binding sites on the protein for all of them [19, 20, 21, 22, 23]. Observed binding stoichiometries in conjunction with X-ray crystallography, Mössbauer, and EPR spectroscopy suggest several types of binding sites, at least one of which is located inside the three-fold channels [3, 6, 24, 25, 26]. Other classes of binding sites involving the ferroxidation and nucleation sites, the external surface of the apoprotein, residues such as His118, His128, Cys130, and other carboxyl groups within the protein shell, have also been identified or proposed as loci for metal ion binding [11, 24, 27, 28, 29, 30].

Zinc and terbium, among other metal ions, are known to interfere with iron deposition in ferritins and to inhibit core formation [20, 25, 26, 27, 28, 29, 31, 32]. They have often been used to probe Fe(II) binding and oxidation in these proteins [25, 33, 34]. Zn(II) exhibits either competitive, non-competitive, or mixed inhibition of O₂ uptake during iron(II) oxidation in ferritins [27, 35]. Such complex behavior has been attributed to the multiple binding sites on ferritin for this metal [27]. X-ray crystallography of the Tb(III) derivative of HuHF has located three terbium binding sites on the protein, two involving A and B sites of the ferroxidase center and a third site C nearby, postulated to be a nucleation site for formation of the ferrihydrite mineral core [19, 36]. In HoSF, up to five binding sites with low and high affinities for Zn(II) and Tb(III) have been identified per ferritin subunit [23, 24, 31]. The identify of the sites primarily responsible for affecting iron uptake by the protein and the affinity of these sites for Zn(II) and Tb(III) remain unresolved.

Besides its use in inhibition studies of iron uptake by ferritin in vitro [20, 25, 33, 34] and in the X-ray crystallographic structure analysis of the protein [37], zinc, like iron, has been found associated with ferritin in vivo. Significant amounts of zinc have been found in ferritins from the tropical rock oyster (*S. cucullata*) [38] and also in partially purified ferritin from rats [39, 40]. The effect of high-Zn diets on Fe metabolism in rats resulted in the formation of a Fe-poor ferritin,

indicating that Zn may interfere with Fe incorporation into ferritin in vivo [40]. It has been suggested that ferritin may function as a zinc detoxification protein and also as a metal storage and transferring agent for both Fe and Zn [41].

Isothermal titration calorimetry (ITC) has been shown to be a very useful technique for measuring metal ion binding to amino acids, peptides, and proteins in solutions [18, 42, 43]. As an extension of our recent ITC investigation on Fe(II) binding to HuHF and its variants [18], we report here a complete thermodynamic study of Zn(II) and Tb(III) binding to HuHF, site-directed variants of HuHF, and human L-chain ferritin (HuLF). The inhibition of Fe(II) binding and oxidation in ferritin is also examined. The results demonstrate that the three-fold channels are the principal binding sites for Zn(II) and Tb(III) in human ferritins. The ferroxidase centers and nucleation sites are also shown to be binding sites for these metal ions, albeit with lower affinity. Fe(II) oxidation activity in ferritin is abolished by one Zn(II) or one Tb(III) binding in each of the three-fold channels, indicating that the mechanism of inhibition occurs through blocking the passage of Fe(II) to the ferroxidase center.

Materials and methods

All chemicals, Mes and Mops buffers (Research Organics), ferrous sulfate heptahydrate, FeSO₄·7H₂O (J.T. Baker), zinc sulfate heptahydrate, ZnSO₄·7H₂O (Mallinckrodt), sodium hydrosulfite, Na₂S₂O₄, and 2,2'-bipyridyl (Aldrich), were of reagent grade and were used without further purification. Terbium standard (10,000 µg/mL) was of reagent ULTRAGrade from Ultra Scientific. Recombinant L-chain and H-chain ferritins and all H-chain variants were prepared as previously described [44, 45] and rendered iron free by dialysis against sodium hydrosulfite (dithionite), Na₂S₂O₄, and complexation with 2,2'-bipyridyl at pH 6.0 [46]. Protein concentrations were determined using the Advanced Protein Assay (<http://Cytoskeleton.com>, patent pending), or spectrophotometrically using the molar absorptivities of 23,000 cm⁻¹ M⁻¹ on a 24mer basis at 280 nm for the H-chain apoprotein [47] and 18,500 cm⁻¹ M⁻¹ at 280 nm for the L-chain apoferritin (present work).

ITC measurements were carried out at 25.00 °C with an upgraded CSC model 4200 isothermal titration calorimeter (Calorimetry Science Corporation, Provo, Utah). The enthalpy change, ΔH , the binding constant, K , and the stoichiometry of binding, n , were determined from a single ITC experiment. From these values, the standard Gibbs free energy change, ΔG° , and standard entropy change, ΔS° , were calculated, and hence all thermodynamic parameters defined. The instrument operation, settings, and calibration were performed as described elsewhere [18]. The data were collected automatically and analyzed with BindWorks 3.0 fitting program (Calorimetry Science). A background experiment using the buffer solution alone was performed to correct for the heats of mixing and dilution. Each protein was titrated two to three times to ensure reproducibility. The errors given in the tables from curve fitting are from replicate measurements. Conditions for each experiment are given in the figure captions.

Spectrophotometric experiments were performed on a Cary 50 Bio UV-visible spectrophotometer. Solutions of standard terbium (62.9 mM, 10,000 µg/mL in dilute HNO₃) and zinc sulfate (0.39–2 mM, pH 7.0) were freshly prepared prior to each experiment and microliter additions of each metal ion solution were made to each

protein sample. The protein solution (1.2 μM) was incubated with different amounts of Zn(II) or Tb(III) (0–20 μM) for 5–10 min at 25 $^{\circ}\text{C}$ with continuous stirring before adding Fe(II) aerobically. The kinetics of iron(II) oxidation and associated Fe(III) mineralization were monitored by the change in absorbance at 305 nm until no further increase was apparent.

Results

ITC studies of Tb(III) binding to HuHF and its variants

Figure 1A shows the raw ITC data for a titration of apoHuHF with Tb(III) in Mops buffer, pH 7.0. The integrated heats for each injection are shown after subtraction of the control injection in buffer alone. The negative peaks seen in Fig. 1A correspond to an endothermic reaction for Tb(III) binding to the protein.¹ The experimental thermodynamic parameters obtained from the curve fitting of the integrated heats in Fig. 1B to a model of two sets of multiple independent binding sites are compiled in Table 1. At least two classes of binding sites, strong ($n_1 \approx 8-9$) and weak ($n_2 \approx 87$) are evident.

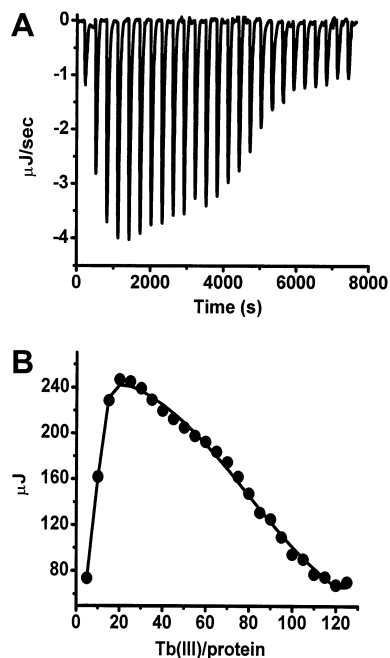


Fig. 1A, B Calorimetric titration of HuHF with Tb(III). **A** Raw data; **B** plot of the integrated heat versus the Tb(III)/protein molar ratio. Conditions: 1.5 μM HuHF titrated with 10 μL injections of 0.975 mM Tb(III). Both protein and Tb(III) are in 100 mM Mops buffer, 50 mM NaCl, pH 7.03, and 25.00 $^{\circ}\text{C}$

¹The sign of the heats in the figures are given relative to the CSC isothermal titration calorimeter. Negative and positive measured heats correspond to endothermic and exothermic binding reactions, respectively

Table 1 Best fit parameters for ITC measurements of Tb^{3+} binding to HuHF and its variants in 0.1 mM Mops buffer, 50 mM NaCl, pH 7.0, 25.00 $^{\circ}\text{C}$ ^a

Protein ^b	n_1	K_1 (M^{-1})	ΔH_1° (kJ/mol)	ΔG_1° (kJ/mol) ^c	ΔS_1° (J/mol K) ^d	n_2	K_2 (M^{-1})	ΔH_2° (kJ/mol)	ΔG_2° (kJ/mol) ^c	ΔS_2° (J/mol K) ^d
HuHF (Fig. 1)	8.77 \pm 0.51	(6.14 \pm 2.49) $\times 10^6$	4.51 \pm 0.89	-38.74 \pm 1.05	145.06 \pm 1.37	87.32 \pm 2.42	(6.68 \pm 1.06) $\times 10^4$	25.41 \pm 1.23	-27.54 \pm 0.39	177.59 \pm 1.29
A2	8.33 \pm 0.26	(6.19 \pm 1.39) $\times 10^6$	5.15 \pm 0.62	-38.76 \pm 0.55	147.27 \pm 0.83	61.43 \pm 1.06	(5.19 \pm 1.35) $\times 10^4$	22.35 \pm 1.22	-26.91 \pm 0.64	165.21 \pm 1.37
222 (Fig. 2)	8.67 \pm 1.09	(1.35 \pm 0.61) $\times 10^6$	5.43 \pm 2.27	-34.99 \pm 1.12	135.56 \pm 2.53	45.61 \pm 2.76	(7.96 \pm 1.87) $\times 10^4$	23.37 \pm 2.95	-27.97 \pm 0.58	172.19 \pm 3.00
S10 (Fig. 4)	7.71 \pm 0.28	(6.02 \pm 2.05) $\times 10^6$	14.81 \pm 0.21	-38.69 \pm 0.84	179.43 \pm 0.86	84.22 \pm 2.85	(1.10 \pm 0.25) $\times 10^4$	31.18 \pm 2.84	-23.06 \pm 0.56	181.92 \pm 2.89
S9	8.13 \pm 0.34	(5.26 \pm 1.15) $\times 10^6$	15.23 \pm 0.64	-38.36 \pm 0.54	179.74 \pm 0.84	81.18 \pm 7.42	(5.51 \pm 1.75) $\times 10^4$	28.76 \pm 2.18	-27.06 \pm 0.78	187.22 \pm 2.31
S14 (Fig. 3)	-	-	-	-	-	43.10 \pm 0.48	(1.28 \pm 0.09) $\times 10^5$	19.33 \pm 0.29	-29.15 \pm 0.17	162.61 \pm 0.33
HuLF (Fig. 5)	9.16 \pm 0.94	(3.40 \pm 1.59) $\times 10^6$	7.14 \pm 1.17	-37.28 \pm 1.16	148.98 \pm 1.64	30.54 \pm 2.41	(1.07 \pm 1.52) $\times 10^5$	15.97 \pm 1.35	-28.71 \pm 3.52	149.85 \pm 4.00

^aThe reported thermodynamic quantities are apparent values and include the contributions to the overall equilibrium from ferritin and buffer species in different states of protonation. Standards errors from replicate determinations are indicated

^bA2, nucleation site variant (E61A + E64A + E67A); S14, three-fold channel variant (D131I + E134F); 222, ferroxidase center variant (E62K + H65G and also K86Q); S9, outer opening to three-fold channel variant (H118A, K86Q); S10, inner opening to three-fold channel variant (H128A, K86Q)

^cCalculated from $\Delta G^{\circ} = -RT \ln K$

^dCalculated from $\Delta S^{\circ} = (\Delta H^{\circ} - \Delta G^{\circ})/T$

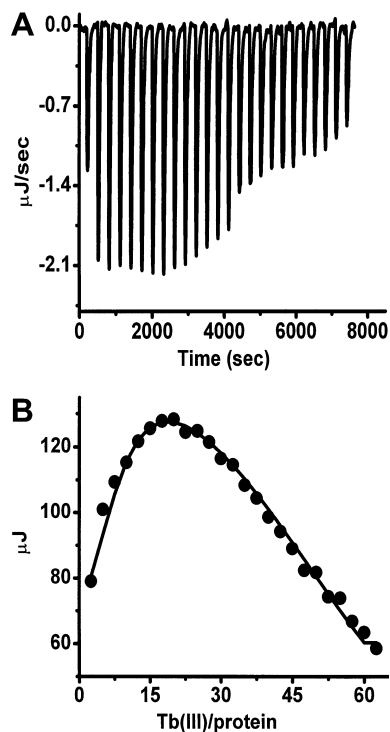


Fig. 2A, B Calorimetric titration of the ferroxidase variant 222 (E62K + H65G and also K86Q) with Tb(III). **A** Raw data; **B** plot of the integrated heat versus the Tb(III)/protein molar ratio. Conditions: 2 μ M protein titrated with 10 μ L injections of 0.65 mM Tb(III). Both protein and Tb(III) are in 100 mM Mops buffer, 50 mM NaCl, pH 7.02, and 25.00 $^{\circ}$ C

Tb(III) binding to ferroxidase site, nucleation site, and channel variants 222, A2, and S14

To establish the loci of Tb(III) binding to HuHF, ITC experiments were carried out using ferroxidase site variant 222 (E62K + H65G + K86Q), nucleation site variant A2 (E61A + E64A + E67A), and three-fold channel variant S14 (D131I + E134F). The double substitution of two ferroxidase site ligands, Glu62 and His65 in variant 222, does not affect the stoichiometry of the first class of strong binding sites ($n_1 \approx 8-9$), but eliminates some of the weak binding of Tb(III) ($n_2 \approx 46$) compared to the wild-type protein ($n_2 \approx 87$) (Fig. 2, Table 1). This result suggests that some of the weak binding sites [about 41 Tb(III) per 24mer, ~ 2 Tb(III)/subunit] involves Tb(III) binding at the ferroxidase center. In variant 222, the binding constant K_1 for the strong sites is smaller by a factor of four when compared to the wild-type HuHF (Table 1).

A titration of the nucleation site variant A2 (not shown) resulted in thermodynamic parameters very similar to those of HuHF for the first class of strong sites [~ 8 Tb(III)/molecule], but reduced binding stoichiometries for the weakest sites compared to the wild-type HuHF [$n_2 \approx 61$ Tb(III)/A2 versus 87 Tb(III)/HuHF, Table 1]. This reduction in the binding stoi-

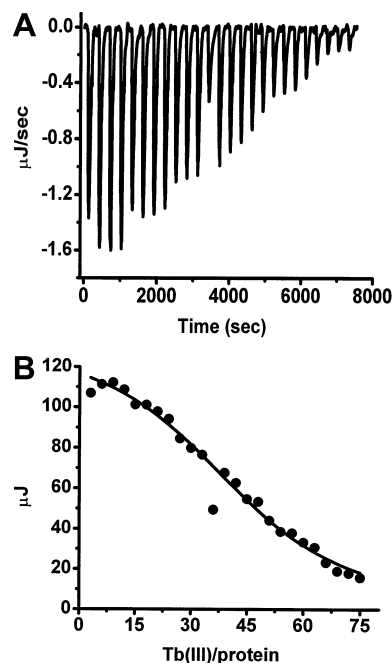


Fig. 3A, B Calorimetric titration of the three-fold channel variant S14 (D131I + E134F) with Tb(III). **A** Raw data; **B** plot of the integrated heat versus the Tb(III)/protein molar ratio. Conditions: 1.5 μ M protein titrated with 10 μ L injections of 0.585 mM Tb(III). Both protein and Tb(III) are in 100 mM Mops buffer, 50 mM NaCl, pH 7.02, and 25.00 $^{\circ}$ C

chiometry for the weak class of binding sites in variant A2 corresponds to ~ 1 Tb(III)/subunit. The loss of one Tb(III) ions per subunit in variant A2 from mutation of the nucleation site ligands (Glu61, Glu64, and Glu67) near the ferroxidase center suggests that the nucleation site C constitutes a weak binding site for terbium. It is also possible that the mutation of Glu61 in variant A2, a shared residue between the B site of the ferroxidase center and the nucleation C site, is the cause of this reduction in binding.

Mutation of the three-fold channel residues in variant S14 (D131I + E134F) totally eliminated the first class ($n_1 \approx 8$) of strong binding (Fig. 3, Table 1), a result indicating that the eight three-fold channels are the probable sites for strong Tb(III) binding to the protein. This mutation also reduces the stoichiometry of weak binding, n_2 , from ~ 87 to ~ 43 Tb(III)/protein (Table 1).

Tb(III) binding to variants S9 and S10

To further identify the specific binding sites on the protein for Tb(III), two additional site-directed variants of HuHF were investigated, variant S9 (H118A) and variant S10 (H128A). Previous spectroscopic studies have suggested the involvement of histidine residues near the outer (S9) and inner (S10) openings of the three-fold channels, in metal ion binding [30, 48, 49].

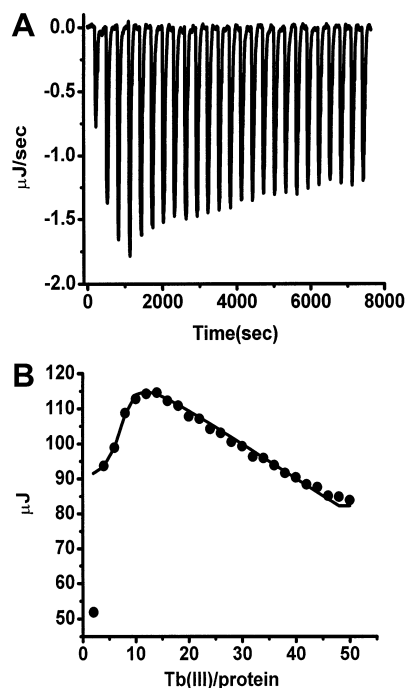


Fig. 4A, B Calorimetric titration of variant S10 (H128A, K86Q) with Tb(III). **A** Raw data; **B** plot of the integrated heat versus the Tb(III)/protein molar ratio. Conditions: 2 μ M protein titrated with 10 μ L injections of 0.52 mM Tb(III). Both protein and Tb(III) are in 100 mM Mops buffer, 50 mM NaCl, pH 7.04, and 25.00 $^{\circ}$ C

Both residues are in close proximity of either Asp131 or Glu134 residues (3–7 \AA), located within the three-fold channel [19, 30]. Figure 4 shows the raw ITC data titration of variant (S10) with Tb(III) and the integrated heats. A similar titration curve was obtained with variant S9 (data not shown). The similarity between the thermodynamic parameters of variants S9, S10, and HuHF (Table 1) eliminates the two residues, His118 and His128, as strong ligands for Tb(III). However, the enthalpies of binding for the strong sites in variants S9 and S10 are about three times higher than that seen with HuHF (Table 1).

Tb(III) binding to HuLF

ITC binding experiments were also performed with Tb(III) and recombinant human L-chain ferritin. Figure 5 shows the raw ITC data for Tb(III) binding to HuLF at pH 7.0 and the integrated heats (μ J) for each injection versus the molar ratio of Tb(III) to the apo-protein. An endothermic reaction is seen and a good fit of the data (Fig. 5B) is achieved using a model with two sets of independent binding sites. As with HuHF, both strong and weak binding classes are observed with HuLF (Fig. 5, Table 1). The stoichiometry of the strong binding class is \sim 8 molar equivalents per protein (Table 1), consistent with the binding of one terbium per three-fold channel. The stoichiometry $n_2 \sim$ 30 of the

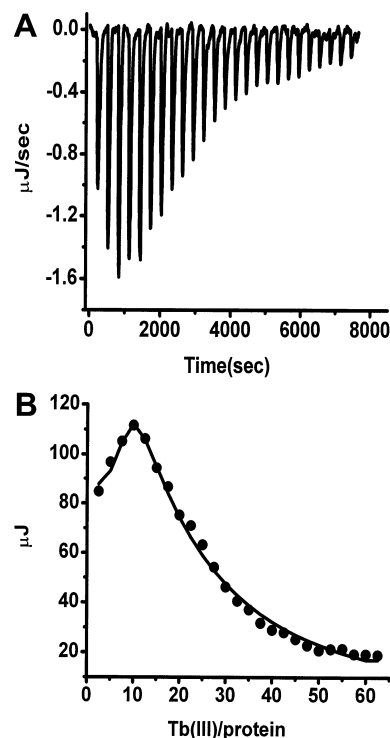


Fig. 5A, B Calorimetric titration of HuLF with Tb(III). **A** Raw data; **B** plot of the integrated heat versus the Tb(III)/protein molar ratio. Conditions: 2 μ M HuLF titrated with 10 μ L injections of 0.65 mM Tb(III). Both protein and Tb(III) are in 100 mM Mops buffer, 50 mM NaCl, pH 7.03, and 25.00 $^{\circ}$ C

second weak class of binding sites seen with HuLF is only \sim 30% of that of the wild-type HuHF.

ITC studies of Zn(II) binding to HuHF and its variants

The ITC data for Zn(II) binding to HuHF in Mops buffer at pH 7.0 are shown in Fig. 6. The heats at the end of the titration were in excess of the heat of dilution (Fig. 6A), indicating some weak binding to the protein. A model of two sets of independent binding sites, strong and weak, was again used to fit the data. The individual thermodynamic parameters of the second class of weak binding sites have inherently large uncertainties as their values are derived from the equation for two classes of binding sites close to its limiting form for weak binding (Table 2) [18, 50]. However, the values of n_1 and n_2 for Zn(II) binding correspond closely to those for Tb(III) binding (cf. Tables 1 and 2). The first class of binding sites in HuHF has a strong affinity for Zn(II) and corresponds to \sim 8 molar equivalent per protein (Fig. 6B, Table 2).

Several site-directed variants of HuHF were used to confirm the specific identities of Zn(II) binding sites on the protein, similar to what was done with Tb(III). Channel variants S9 (H118A) (Fig. 7A) and S10 (H128A) (titration not shown) show titration curves and thermodynamic parameters similar to those of the wild-type HuHF (Table 2). The results indicate the presence

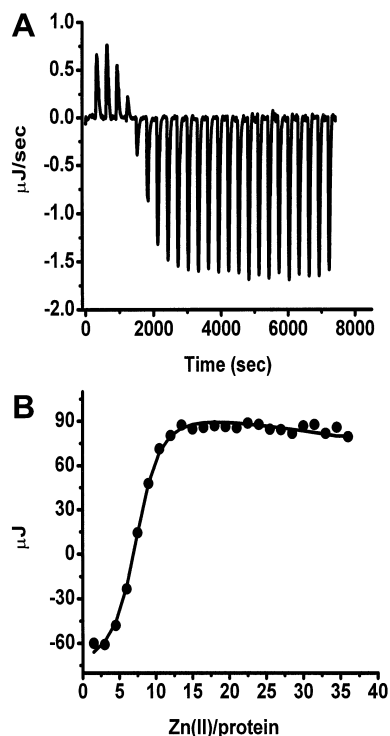


Fig. 6A, B Calorimetric titration of HuHF with Zn(II). **A** Raw data; **B** plot of the integrated heat versus the Zn(II)/protein molar ratio. Conditions: 3 μ M HuHF titrated with 10 μ L injections of 0.58 mM Zn(II). Both protein and Zn(II) are in 100 mM Mops buffer, 50 mM NaCl, pH 7.04, and 25.00 $^{\circ}$ C

of two classes of binding sites, one strong [\sim 8 Zn(II)/shell] and the other weak [\sim 91 Zn(II)/shell] (Table 2).² Substitution of Asp131 and Glu134 residues within the three-fold channel in variant S14 (D131I+E134F) eliminates the strong binding class of Zn(II) while conserving some of the other weak binding sites on the protein (Table 2; see Discussion).

The ferroxidase center variant 222 and nucleation site variant A2 of HuHF were also tested for the potential involvement of these sites in Zn(II) binding. Variant A2 shows a similar Zn(II) titration curve as that for HuHF (titration not shown; Table 2). The strong class of binding sites in A2 corresponds to the binding of \sim 8 molar equivalents of Zn(II) per protein, consistent with binding in the three-fold channel [1 Zn(II)/channel]. However, the second class of sites corresponds to weak binding of Zn(II) with reduced stoichiometry of \sim 64 Zn(II)/protein (Table 2), similar to $n_2 \approx 61$ for Tb(III) binding to A2 (Table 1), and compared to $n_2 \approx 91$ for Zn(II) binding to HuHF. The results from variant 222

²Because of the large errors associated with the stoichiometries obtained for the second class of binding sites (Table 2), we cannot exclude the possibility that the histidine residues (namely His118 and His128) are weak binding ligands for either Zn(II) or Tb(III). Attempts using higher protein and ligand concentration to more accurately determine the stoichiometry of this second class of weak sites were unsuccessful. A small amount of precipitation and/or cloudy solutions were observed under these conditions

Table 2 Best fit parameters for ITC measurements of Zn²⁺ binding to HuHF and its variants in 0.1 mM Mops buffer, 50 mM NaCl, pH 7.0, 25.00 $^{\circ}$ C^a

Protein ^b	n_1	K_1 (M ⁻¹)	ΔH_1° (kJ/mol)	ΔG_1° (kJ/mol) ^c	ΔS_1° (J/mol K) ^d	n_2	K_2 (M ⁻¹)	ΔH_2° (kJ/mol)	ΔG_2° (kJ/mol) ^c	ΔS_2° (J/mol K) ^d
HuHF (Fig. 6)	6.91 \pm 0.17	(5.96 \pm 1.67) $\times 10^6$	-13.48 \pm 0.53	-38.67 \pm 0.69	84.48 \pm 0.87	90.66 \pm 29.46	(3.09 \pm 0.65) $\times 10^4$	22.12 \pm 5.49	-25.62 \pm 0.52	160.12 \pm 5.51
A2	9.34 \pm 0.17	(5.37 \pm 1.78) $\times 10^6$	-15.63 \pm 0.21	-38.41 \pm 0.82	76.40 \pm 0.85	64.33 \pm 35.17	(8.73 \pm 1.17) $\times 10^3$	21.19 \pm 1.95	-22.49 \pm 0.33	146.50 \pm 1.97
222	8.91 \pm 1.48	(3.12 \pm 0.73) $\times 10^6$	-15.76 \pm 1.74	-37.06 \pm 0.58	71.44 \pm 1.83	46.64 \pm 4.06	(6.59 \pm 2.27) $\times 10^4$	23.15 \pm 3.97	-27.51 \pm 0.85	169.91 \pm 4.06
S10	8.27 \pm 0.13	(8.48 \pm 1.15) $\times 10^6$	-20.83 \pm 0.38	-39.54 \pm 0.33	62.75 \pm 0.51	94.51 \pm 26.91	(3.74 \pm 1.92) $\times 10^3$	24.22 \pm 4.45	-20.39 \pm 1.27	149.62 \pm 4.62
S9 (Fig. 7)	9.82 \pm 0.13	(3.11 \pm 0.39) $\times 10^6$	-23.37 \pm 0.47	-37.06 \pm 0.31	45.92 \pm 0.56	87.58 \pm 36.88	(6.87 \pm 1.65) $\times 10^3$	20.64 \pm 3.09	-21.90 \pm 0.59	142.68 \pm 3.14
S14	-	-	-	-	-	43.66 \pm 0.63	(7.51 \pm 0.64) $\times 10^4$	11.59 \pm 0.27	-27.83 \pm 0.21	132.21 \pm 0.34
HuLF	7.46 \pm 0.79	(1.05 \pm 0.15) $\times 10^5$	-12.98 \pm 4.99	-28.66 \pm 0.35	52.59 \pm 5.00	15.85 \pm 1.78	(2.96 \pm 0.32) $\times 10^4$	33.17 \pm 5.51	-25.52 \pm 0.27	196.84 \pm 5.51

^aThe reported thermodynamic quantities are apparent values and include the contributions to the overall equilibrium from ferritin and buffer species in different states of protonation. Standards errors from replicate determinations are indicated

^bA2, nucleation site variant (E61A + E64A + E67A); S14, three-fold channel variant (D131I + E134F); 222, ferroxidase center variant (E62K + H65G and also K86Q); S9, outer opening to three-fold channel variant (H118A, K86Q); S10, inner opening to three-fold channel variant (H128A, K86Q)

^cCalculated from $\Delta G^{\circ} = -RT \ln K$

^dCalculated from $\Delta S^{\circ} = (\Delta H^{\circ} - \Delta G^{\circ})/T$

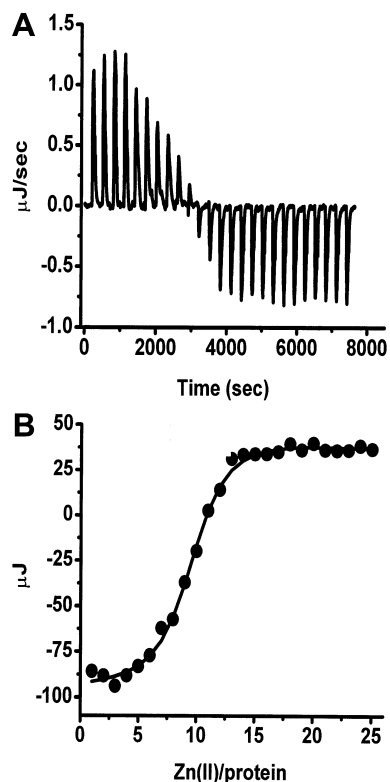


Fig. 7 Calorimetric titration of variant S9 (H118A, K86Q) with Zn(II). **A** Raw data; **B** plot of the integrated heat versus the Zn(II)/protein molar ratio. Conditions: 3 μ M protein titrated with 10 μ L injections of 0.39 mM Zn(II). Both protein and Zn(II) are in 100 mM Mops buffer, 50 mM NaCl, pH 7.04, and 25.00 $^{\circ}$ C

indicate the presence of a strong class of binding sites [\sim 8 Zn(II) shell, Table 2] and a reduced binding stoichiometry for the second class of weak sites [\sim 46 Zn(II)/shell]. Taken together, the data for variants A2 and 222 imply that the nucleation and ferroxidase sites are among the weak sites for Zn(II) binding in HuHF (Table 2).

Zn(II) binding to HuLF

Zn(II) binding to HuLF was also examined (Table 2). Similar to what has been observed with HuHF and its variants, Zn(II) binding to HuLF indicates the presence of strong and weak classes of binding sites, with $n_1 \approx 8$ and $n_2 \approx 15$ Zn(II)/HuLF (Table 2).

Kinetic studies of Fe(II) oxidation in HuHF in the presence of Zn(II) and Tb(III)

Kinetic measurements were undertaken to relate the thermodynamic data obtained from ITC measurements to the inhibition effects of Tb(III) and Zn(II) on Fe(II) oxidation in ferritin. Figure 8A shows the initial rate of Fe(II) oxidation versus the ratio of Tb(III) per protein molecule when 48 Fe(II) were added to the apoprotein following Tb(III) addition. Iron oxidation/mineralization

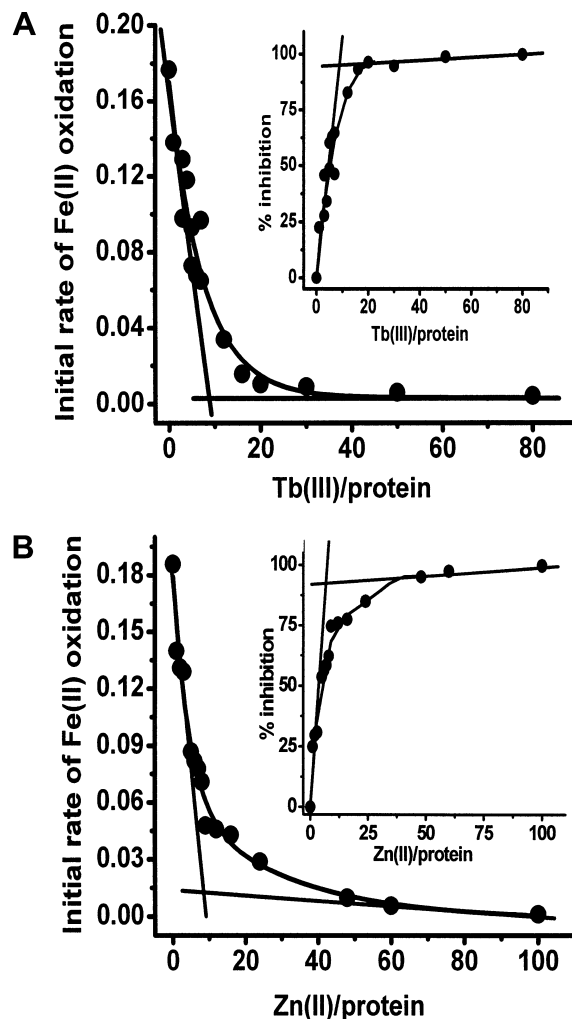


Fig. 8A, B Kinetics of Fe(II) oxidation in HuHF. **A** Dependence of the initial rate of Fe(II) oxidation on the Tb(III)/protein ratio. *Inset*: percent inhibition of the initial rates versus Tb(III)/protein ratio. **B** Dependence of the initial rate of Fe(II) oxidation on the Zn(II)/protein ratio. *Inset*: percent inhibition of the initial rates versus Zn(II)/protein ratio. Conditions: 2.0 μ M HuHF, 100 mM Mops, 50 mM NaCl, pH 7.0, 25.0 $^{\circ}$ C. Fresh solutions of 2 mM Tb(III) or Zn(II) were first added to give different metal/HuHF ratios followed by 48 Fe(II)/protein as 32 mM FeSO₄, 5–10 min later in air. Each data point represents a different protein sample

inhibition occurs with a stoichiometry of 8 Tb(III)/HuHF, consistent with one Tb(III) binding in each of the eight hydrophilic three-fold channels and blocking access of Fe(II) to the inside of the protein shell where oxidation at the ferroxidase centers occurs. Similar results were obtained when Zn(II) was added to the protein prior to the addition of Fe(II) (Fig. 8B). Inhibition again occurs with a stoichiometry of 8 Zn(II)/HuHF.

Discussion

The results of this study indicate that Zn(II) and Tb(III) have common binding sites in both H- and L-subunits. The site-directed mutagenesis experiments with H-chain

ferritin reveal the identity of these binding sites and indicate that the three-fold channels are the primary sites for strong Zn(II) and Tb(III) binding. Weaker binding at the ferroxidase and nucleation sites is suggested from the binding stoichiometries in Tables 1 and 2. Previous kinetic experiments using electrode oximetry have shown that Zn(II) exhibits non-competitive inhibition of Fe(II) oxidation at low Zn(II) concentrations, consistent with binding in the channels, and competitive inhibition at high Zn(II) concentration, consistent with occupancy of the ferroxidase sites as found here [27]. The ITC data not only demonstrate the presence of two classes of binding sites, but identify the location of these sites and provide the thermodynamic parameters for the Zn(II) and Tb(III) interactions with these sites.

The residues that line the hydrophilic three-fold channel (Asp131, Glu134, His118, and His128) are conserved between H- and L-chain ferritins. In the first class of binding sites, the stoichiometries of ~ 8 Tb(III) or ~ 8 Zn(II) per ferritin molecule obtained with HuHF, its variants with unaltered channels, and with HuLF are in accord with binding in the eight hydrophilic three-fold channels, one Tb(III) or one Zn(II) per channel in all proteins (Tables 1 and 2). This assignment is consistent with the results for the three-fold channel variant S14, where mutation of the ligands Asp131 and Glu134 totally eliminates the first class of Tb(III) and Zn(II) binding sites (Fig. 3, Tables 1 and 2). In addition, the thermodynamic parameters, ΔH° , ΔS° , and ΔG° for this first class of $n_1 \approx 8$ binding sites for Zn(II) and Tb(III) are similar for HuHF and HuLF, consistent with common binding sites in both proteins.

That 8 Tb(III)/shell or 8 Zn(II)/shell greatly reduce the rate of Fe(II) oxidation in HuHF (Fig. 8) is further strong evidence that these metal ions bind in the three-fold channels of the protein and hinder the access of iron(II) to the ferroxidase centers via the channels, the main pathway of Fe(II) to these centers [11, 12, 13, 14, 15, 16, 17, 18, 51]. Consistent with these observations, Zn(II) and Tb(III) have been previously shown UV-fluorescence and X-ray crystallography to bind in the three-fold channel of HoSF and HuHF and form stable complexes [11, 21, 22, 24].

While all the ferritins investigated here show the same binding stoichiometries ($n_1 \approx 8$) for the first class of strong binding sites (Tables 1 and 2), the stoichiometries for the second class of weak binding sites differ. A stoichiometry of ~ 90 metal ions per molecule is obtained when S9 (His118A), S10 (His128A), or the wild-type HuHF are titrated with either Tb(III) or Zn(II). It is evident that neither His118 nor His128 is a strong ligand for Tb(III) or Zn(II) and that their mutation does not eliminate the binding of these metal ions in the hydrophilic three-fold channel of human ferritin but does increase the binding enthalpies (Tables 1 and 2).

The reduction in the n_2 stoichiometries of the ferroxidase site variant 222 compared to HuHF implies that the ferroxidase sites constitute some of the weak binding sites on the protein (Tables 1 and 2). The n_2 values

indicate that about two metal ions per subunit are lost with variant 222, consistent with the binding of 2 Tb(III) or Zn(II) per ferroxidase center. This same situation is observed with the nucleation site variant A2, where the weak binding of ~ 24 Zn(II) or Tb(III) is eliminated by the mutation, an indication that the nucleation site ligands are also probably involved in the binding of one Tb(III) or Zn(II) per subunit (Tables 1 and 2). Thus, the ITC results are in accord with the X-ray crystallography of the Tb(III) derivative of HuHF showing the presence of three terbium ions, two at the ferroxidase sites A and B and one at the nucleation site C of the protein [19]. The reduced number of weak binding sites for Zn(II) and Tb(III) in HuLF compared to HuHF is consistent with HuLF lacking a ferroxidase site and having only 55% homology in sequence with HuHF [52].

In the case of Tb(III) binding to HuHF, ITC titrations reveal two endothermic binding events, $\Delta H^\circ = 4.5$ and 25.4 kJ/mol, respectively (Table 1). In contrast, titrations of HuHF and its variants with Zn(II) first show an exothermic event followed by an endothermic event, $\Delta H^\circ = -13.5$ and 22.1 kJ/mol, respectively (Table 2). Variable enthalpies and entropies for the strong and the weak interaction with both Zn(II) and Tb(III) are observed, depending on the protein (Tables 1 and 2). However, the large positive entropy values obtained in all cases indicate that the binding interactions are primarily entropically driven, as previously observed with Fe(II) binding to HuHF [18]. These favorable entropies are most likely due to the change in the hydration of the protein and of the metal ions upon binding, thereby releasing H₂O into the bulk solution. Strong binding to the first class of Zn(II) sites is achieved by both favorable enthalpy and entropy changes (Table 2).

The different ΔH_1° and ΔS_1° values for the interaction of Tb(III) or Zn(II) with variants S9 and S10 when compared to either HuHF or HuLF (Tables 1 and 2) is likely due to some structural modification in the region of the mutations that influences binding in the channels. Similar mutational effects inducing conformational changes and secondary structure destabilization have been previously observed in these variants [30, 53]. In addition, while the stoichiometry remains at $n_1 \approx 8$ for the binding in the three-fold channels, the equilibrium constant K_1 for Zn(II) or Tb(III) binding is influenced by mutations elsewhere in the protein. K_1 for Tb(III) and Zn(II) binding to the ferroxidase site variant 222 is reduced fivefold and twofold over that of HuHF (Tables 1 and 2). Binding of both Tb(III) and Zn(II) in the channels of HuLF also occurs with lower affinity than seen with HuHF and is 60 times weaker in the case of Zn(II) binding (Table 2). These data indicate that structural changes associated with amino acid substitutions in one part of the protein influence the strength of metal binding elsewhere.

In conclusion, the present study provides further insight into the location of the strong and weak binding sites for different metal ions in ferritin. Zn(II) and Tb(III) strongly bind in the three-fold channels of ferritin,

inhibiting the access of Fe(II) to the ferroxidase centers, the main pathway for iron oxidation and core mineralization. The ferroxidase and nucleation sites are also shown to be binding sites for zinc and terbium, albeit with lower affinity. The data further indicate the presence of other weak binding sites on the protein. HuLF, lacking ferroxidase sites, has significantly fewer weak binding sites for Zn(II) and Tb(III) although the strong binding in the conserved three fold-channels is retained.

Acknowledgements This work was supported by grant R01 GM20194 from the National Institute of General Medical Sciences (N.D.C.), and by MURST-Cofin 2001 and 2002 (P.A.) and CNR-Agenzia 2000 (P.A. and S.L.).

References

- Theil EC (1987) *Annu Rev Biochem* 56:289–315
- Andrews SC (1998) *Adv Microbial Physiol* 40:281–351
- Harrison PM, Arosio P (1996) *Biochim Biophys Acta* 1275:161–203
- Chasteen ND (1998) In: Sigel H, Sigel A (eds) *Metal ions in biological systems*, vol 35. Dekker, New York, pp 479–514
- Chasteen ND, Harrison PM (1999) *J Struct Biol* 126:182–194
- Levi S, Santambrogio P, Cozzi A, Rovida E, Corsi B, Tamborini E, Spada S, Albertini A, Arosio P (1994) *J Mol Biol* 238:649–654
- Zhao G, Bou-Abdallah F, Arosio P, Levi S, Janus-Chandler C, Chasteen ND (2003) *Biochemistry* 42:3142–3150
- Bou-Abdallah F, Papaefthymiou GC, Scheswohl DM, Stanga SD, Arosio P, Chasteen ND (2002) *Biochem J* 364:57–63
- Moënné-Loccoz P, Krebs C, Herlihy K, Edmondson DE, Theil EC, Huynh BH, Loehr TM (1999) *Biochemistry* 38:5290–5295
- Treffry A, Zhao Z, Quail MA, Guest JR, Harrison PM (1997) *Biochemistry* 36:432–441
- Levi S, Santambrogio P, Corsi B, Cozzi A, Arosio P (1996) *Biochem J* 317:467–473
- Desideri A, Stefanini S, Polizio F, Petruzelli R, Chiancone E (1991) *FEBS Lett* 287:10–14
- Levi S, Luzzago A, Franceschinelli F, Santambrogio P, Cesareni G, Arosio P (1989) *Biochem J* 264:381–388
- Theil EC, Takagi H, Small GW, He L, Tipton AR, Danger D (2000) *Inorg Chim Acta* 297:242–251
- Jin W, Takagi H, Pancorbo B, Theil EC (2001) *Biochemistry* 40:7525–7532
- Yang X, Chasteen ND (1996) *Biophys J* 71:1587–1595
- Yang X, Arosio P, Chasteen ND (2000) *Biophys J* 78:2049–2059
- Bou-Abdallah F, Arosio P, Santambrogio P, Yang X, Janus-Chandler C, Chasteen ND (2002) *Biochemistry* 41:11184–11191
- Lawson DM, Artymiuk PJ, Yewdall SJ, Smith JMA, Livingstone JC, Treffry A, Luzzago A, Levi S, Arosio P, Cesareni G, Thomas CD, Shaw WV, Harrison PM (1991) *Nature* 349:541–544
- Stefanini S, Chiancone E, Antonini E, Finazzi-Agro A (1983) *Arch Biochem Biophys* 222:430–434
- Rice DW, Ford GC, White JL, Smith JMA, Harrison PM (1983) *Adv Inorg Biochem* 5:39–50
- Ford GC, Harrison PM, Rice DW, Smith JMA, Treffry A, White JL, Yarif J (1984) *Phil Trans R Soc Lond Ser B* 304:551–565
- Harrison PM, Lilley TH (1989) In: Loehr TM (ed) *Physical bio-inorganic chemistry*, vol 5. VCH, New York, pp 123–238
- Harrison PM, Ford GC, Rice DW, Smith JMA, Treffry A, White JL (1986) In: Xavier A (ed) *Frontiers in bioinorganic chemistry*. VCH, Weinheim, Germany, pp 268–277
- Treffry A, Bauminger ER, Hechel D, Hodson NW, Nowik I, Yewdall SJ, Harrison PM (1993) *Biochem J* 296:721–728
- Wardeska JG, Viglione B, Chasteen ND (1986) *J Biol Chem* 261:6677–6683
- Sun S, Arosio P, Levi S, Chasteen ND (1993) *Biochemistry* 32:9362–9369
- Chasteen ND, Theil EC (1982) *J Biol Chem* 257:7672–7677
- Macara IG, Hoy TG, Harrison PM (1973) *Biochem J* 135:785–789
- Grady JK, Shao J, Arosio P, Santambrogio P, Chasteen ND (2000) *J Inorg Biochem* 80:107–113
- Treffry A, Harrison PM (1984) *J Inorg Biochem* 21:9–20
- Treffry A, Banyard SH, Hoare RJ, Harrison PM (1977) In: Brown E, Aisen P, Fielding J, Crichton RR (eds) *Proteins of iron metabolism*. Grune & Stratton, New York, pp 3–11
- Treffry A, Zhao Z, Quail MA, Guest JR, Harrison PM (1998) *J Biol Inorg Chem* 3:682–688
- Bauminger ER, Treffry A, Quail MA, Zhao Z, Nowik I, Harrison PM (2000) *Inorg Chim Acta* 297:171–180
- Sun S, Chasteen ND (1992) *J Biol Chem* 267:25160–25166
- Levi S, Yewdall SJ, Harrison PM, Santambrogio P, Cozzi A, Rovida E, Albertini A, Arosio P (1992) *Biochem J* 288:591–596
- Stillman TJ, Hempstead PD, Artymiuk PJ, Andrews SC, Hudson AJ, Treffry A, Guest JR, Harrison PM (2001) *J Mol Biol* 307:587–603
- Webb J, Macey D, Talbot V (1985) *Arch Environ Contam Toxicol* 14:403–407
- Coleman CB, Matrone G (1969) *Biochim Biophys Acta* 177:106–112
- Settlemyre CT, Matrone G (1967) *J Nutr* 92:153–158
- Price D, Joshi JG (1982) *Proc Natl Acad Sci USA* 79:3116–3119
- Zhang Y, Akilesh S, Wilcox DE (2000) *Inorg Chem* 39:3057–3064
- Zhang Y, Wilcox DE (2002) *J Biol Inorg Chem* 7:327–337
- Levi S, Luzzago A, Cesareni G, Cozzi A, Franceschinelli F, Albertini A, Arosio P (1988) *J Biol Chem* 263:18086–18092
- Santambrogio P, Cozzi A, Levi S, Rovida E, Magni F, Albertini A, Arosio P (2000) *Protein Expression Purification* 19:212–218
- Bauminger ER, Harrison PM, Hechel D, Nowik I, Treffry A (1991) *Biochim Biophys Acta* 1118:48–58
- Zhao G, Bou-Abdallah F, Yang X, Arosio P, Chasteen ND (2001) *Biochemistry* 40:10832–10838
- Gerfen GJ, Hanna PM, Chasteen ND, Singel DJ (1991) *J Am Chem Soc* 113:9513–9519
- Hanna PM, Chasteen ND, Rottman GA, Aisen P (1991) *Biochemistry* 30:9210–9216
- Freire E, Mayorga OL, Straume M (1990) *Anal Chem* 62:950A–959A
- Barnés CM, Theil EC, Raymond KN (2002) *PNAS* 99:5195
- Grossman MJ, Hinton SM, Minak-Bernero V, Slaughter C, Stiefel EI (1992) *Proc Natl Acad Sci USA* 89:2419–2423
- Lee M, Arosio P, Cozzi A, Chasteen ND (1994) *Biochemistry* 33:3679–3687